Comprehensive Assessment of Flood Impact, Zonal Statistics, and Site Suitability for Wind Turbines in Iowa

Duran, E. [1,2], Demir, I[1,2,3]

[1] IIHR—Hydroscience and Engineering, University of Iowa, Iowa City, Iowa, USA
[2] Civil and Environmental Engineering, University of Iowa, Iowa City, Iowa, USA
[3] Electrical and Computer Engineering, University of Iowa, Iowa City, Iowa, USA

* Corresponding Author: ege-duran@uiowa.edu

Abstract

Floods, exacerbated by climate change and urban development, pose significant global risks, particularly impacting the wind energy sector in Iowa due to its reliance on wind power. Despite this, current research often overlooks the comprehensive effects of environmental factors on wind turbine vulnerability. This study investigates how elevation and flood risk influence the susceptibility of wind turbines to damage in Iowa. Utilizing Geographic Information Systems (GIS) and statistical analyses, we investigated the likelihood of flooding in designated buffer zones, considering soil drainage capabilities. Additionally, we explored potential disruptions in wind energy capacity and recommended optimal turbine placement sites. Our findings revealed a significant correlation between elevation variations, flood likelihood, and turbine vulnerability, suggesting that larger buffer zones lead to increased exposure to flood risks. These insights underscore the urgent need for proactive mitigation strategies to enhance the resilience of Iowa's renewable energy infrastructure against environmental challenges. This research provides critical knowledge to inform decision-making and safeguard Iowa's wind energy assets against future flood events.

Keywords: Flood Impact, Wind Turbine, Zonal Statistics, Risk Assessment, Energy Infrastructure

1. Introduction

Floods are among the most devastating natural disasters worldwide, and their impact is worsened by climate change, population growth, and rapid urbanization (Sadler et al., 2017; Cikmaz et al., 2023). This global threat causes significant financial losses, displacement, and infrastructure damage (Borowska-Stefańska et al., 2017; McDermott, 2022). In contrast to many other natural disasters, floods usually strike densely populated areas, leading to both immediate and enduring negative effects on communities (Yildirim et al., 2022). These disasters can be triggered by a variety of factors, such as rainfall patterns, severity, and distribution, as well as land cover, soil moisture, and the capacity of stream networks (Lebbe et al., 2014; Li and Demir, 2022).

The unpredictability of floods, characterized by their sudden onset and prolonged duration, ranging from days to potentially weeks depending on terrain and drainage systems, magnifies the challenges of recovery (Duran et al., 2023). Understanding these dynamics is pivotal as our study embarks on unraveling the intricate nexus between topography, flood risk, and wind turbine vulnerability, aiming to fortify Iowa's energy landscape against these threats. The central inquiry driving our investigation is unequivocal: How do variations in elevation and soil drainage capacity influence the susceptibility of wind turbines to floods in Iowa? This question underscores the imperative of comprehending the interplay between natural terrain features and the integrity of wind energy infrastructure, particularly considering the escalating frequency and severity of flooding events (Li et al., 2023a).

The Midwest region of the United States, including Iowa, is one of the most flood-prone areas, as shown by numerous studies (Demir et al., 2022; Sit et al., 2021). Particularly Iowa faces significant flood risks due to its landscape, which is shaped by major waterways like the Mississippi River to the east and the Missouri River to the west (Li et al., 2023b). Historical flood events, especially the major one in 2008, which was one of the largest natural disasters in U.S. history, highlight the state's vulnerability (USGS, 2010; Mutel, 2010). Although there have been several comprehensive studies that explored flood mitigation strategies for Iowa's transportation networks (Alabbad et al., 2023), critical amenities (Grant et al., 2024), and agricultural areas (Tanir et al., 2024), there is still a significant gap in assessing flood risks for energy infrastructures, especially for wind turbines, and this gap highlights the need further research for Iowa wind turbine flood vulnerability.

As fossil fuel reserves such as coal, oil, and gas scarcer and environmental concerns grow, the global economy's expansion and rising energy consumption make it more urgent to find reliable renewable energy alternatives (Martinez & Iglesias, 2021; Zhang et al., 2021; Rezaei-Shouroki, 2017). Wind energy has become a major solution due to its availability and cost-effectiveness, making it one of the fastest-growing power sources worldwide (Grassi et al., 2012; Hou et al., 2022). Recently, no energy sources have impacted electricity generation as much as wind and natural gas, and this has reshaped the energy landscape (Pasqualetti, 2011). This trend is expected to accelerate in the coming decades, with wind power playing a pivotal role in fighting climate change and promoting energy sustainability (Porté-Agel et al., 2020). As wind

energy becomes more important to our electricity supply, it is crucial to ensure the resilience of wind infrastructure, especially in regions prone to flooding.

In this context, Iowa is a crucial case study due to its substantial dependence on wind power and its extensive wind energy resources. The state, well-known for its vast wind farms, faces the dual challenge of utilizing its wind energy resources to the utmost while preserving its vital wind infrastructure from flooding. Iowa is a leader in renewable energy in the US, with over 6,345 wind turbines contributing significantly to the state's energy output (Iowa Environmental Council, 2023). Numerous wind turbines have been installed throughout Iowa, particularly in the northwest and north-central regions, where prevailing winds are most suitable for generating electricity by using wind energy (Gkritza et al., 2010). Since wind energy provides almost two-thirds of the state's energy needs, it is critical to protect this infrastructure from flooding risks (Yildirim et al., 2023). Wind turbines are susceptible to flooding even though they are frequently situated in elevated areas. This emphasizes the necessity of thorough flood impact assessments in order to preserve the stability of Iowa's energy supply.

The existing literature has primarily focused on flood risk and wind turbine performance separately, creating a notable gap in comprehensive research that integrates multiple environmental parameters to assess their combined impacts. Although previous studies have examined flood profiles (Elmousafa et al., 2020), drainage capacity (Jakecemara et al., 2019; Zhou, 2006), and soil characteristics separately (Michael et al., 2018), there are not many integrated methods that assess how these variables interact to affect wind turbine vulnerability. Additionally, there are some feasibility studies for Iowa, with economical and wind performance-based analyses (Grassi et al., 2012; Sanchez Gomez & Lundquist, 2020; Milligan & Factor, 2000), yet none of these studies have integrated flood risk assessments into wind energy infrastructure planning, making this study a crucial step in bridging this gap by addressing the vulnerabilities of wind turbines to flooding.

Our analytical approach employs a range of robust methodologies, including advanced statistical techniques such as correlation analysis, to elucidate the relationships between elevation variance, flood risk, and wind turbine vulnerability. Additionally, we utilize advanced GIS techniques to define buffer zones around wind turbines and analyze spatial data, facilitating a nuanced understanding of terrain characteristics and their association with flood risk. By incorporating flood depth data, we carefully assess the susceptibility of wind turbine locations to flood events, creating a detailed picture of their vulnerability.

The assessment of flood risk is essential for the mitigation of potential damage caused by flooding and the management of flood hazards (Alabbad et al., 2024). Our goal is to address the existing knowledge gap and offer practical solutions to lessen Iowa's wind turbines' susceptibility to flooding. Through a comprehensive examination of the relationship between elevation variance, flood risk, and wind turbine susceptibility, our study aims to pinpoint vulnerable areas and create focused mitigation plans. By utilizing buffer zones surrounding wind turbines and carrying out comprehensive statistical examinations within these zones, our goal is to identify

practical trends that can direct preemptive actions to reduce downtime and guarantee the uninterrupted functioning of wind energy systems during flood incidents.

By translating our research into workable solutions that protect Iowa's renewable energy infrastructure from the effects of flooding, we enhance community resilience and sustainability while simultaneously advancing scientific understanding. We additionally evaluated the possible effects of flooding on Iowa's energy supply, paying particular attention to risks posed by flood events that occur once every 100 and 500 years. We examined how much these scenarios could affect the state's ability to produce energy. We also used data on vacant lands, flood maps, and Iowa's average wind profile to find potential locations for future wind turbine installations. The absence of existing turbines, ideal wind conditions, and flood safety were the selection criteria for these locations. Our objective is to provide a more thorough understanding of the opportunities and challenges associated with wind energy infrastructure in flood-prone areas by taking these factors into account.

The remainder of our study is structured into three main sections: methodology, results and discussion, and conclusion. The methodology section meticulously details our analysis approach, including data preparation, visualization, and the intricate steps of our statistical analysis. In the results and discussion section, we present our findings and explore their implications, providing insights that pave the way for future research endeavors. Finally, the conclusion encapsulates the overarching results and their broader implications, charting a course for further exploration in this critical field.

2. Methodology

This section outlines the process utilized to assess how flooding affects wind turbines and identify potential sites for new installations. In order to evaluate the existing turbines' flood vulnerability, the process starts by defining buffer zones around them. After that, elevation, drainage capacity, and flood depth within these zones are examined. Calculating key metrics like average elevation and its variance aids in understanding how terrain affects turbine risk. The relationships between elevation, flood risk, and turbine vulnerability are investigated through correlation analysis, which identifies the best locations for new turbines based on factors like wind efficiency and flood safety.

2.1. Data Preparation

We obtained the Iowa wind turbine location data from the United States Geological Survey (USGS), and the Iowa Digital Elevation Model (DEM) and HUC8 watershed depth raster from Iowa Geospatial Data Clearinghouse (IGDC). For flood risk data, we used the 100- and 500-year Flood Extension information from both the Iowa Flood Center (IFC) and IGDC. The Iowa Main Soil Profile came from the Iowa State University geographic database. To determine suitable wind turbine locations, we used Multi-year Annual Average wind data from the National Renewable Energy Laboratory. Geographic Information System (GIS) tools were then employed to create Figure 1, which visually represents these datasets.

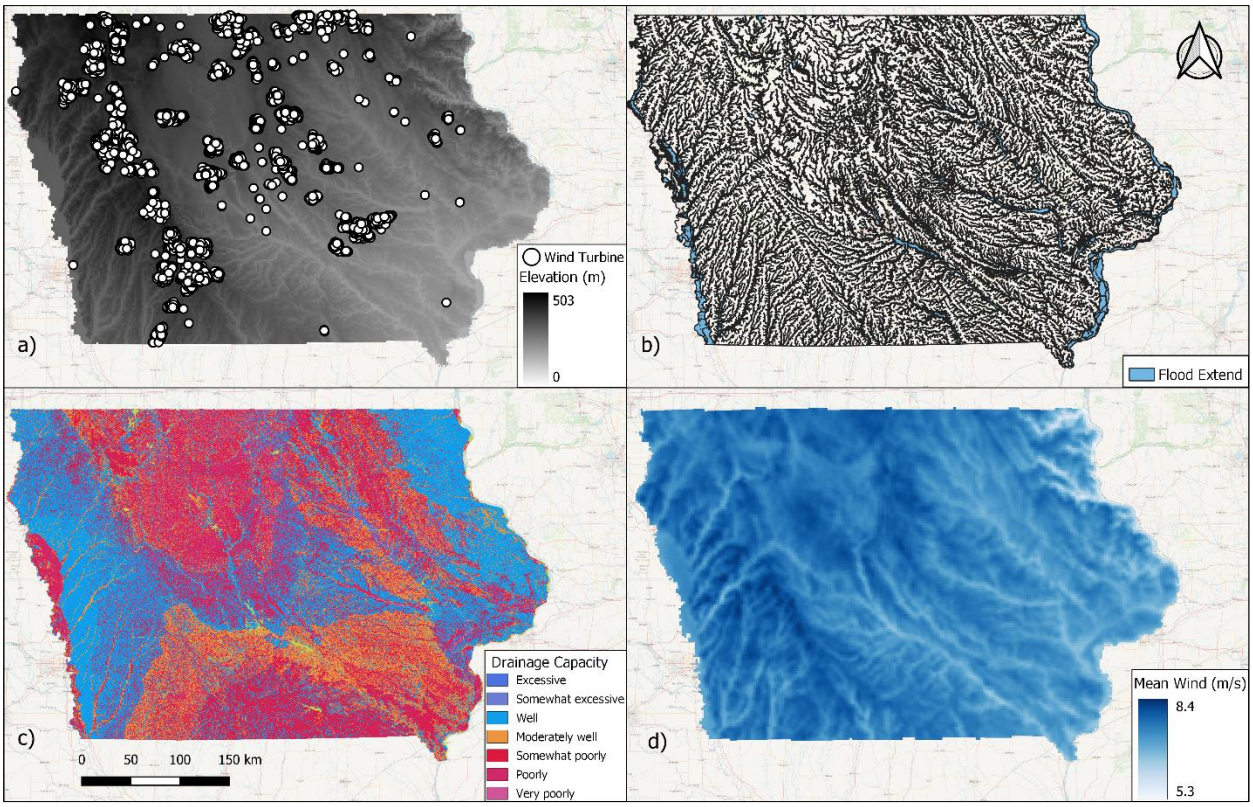

Figure 1. Iowa State database representation: a) wind turbine locations overlaid with the mean elevation profile of Iowa; b) 500-year flood extent map; c) distribution map of drainage capacity; d) annual mean wind profile at 100-meter height.

The physical characteristics of Iowa, particularly in its upper-central and western regions, is conducive to installing wind turbines, as indicated by the USGS dataset in Figure-a. On the other hand, Figure 1-b underscores that flooding risks are present throughout Iowa, indicating that no area in the state is entirely immune from the threat of flood inundation. Also, as can be obtained from Figure 1-a and Figure 1-d, wind turbines are generally placed at elevated locations in order to take advantage of steady wind profiles. As shown in Figure 1c, Iowa's landscape primarily features areas with well-drained and poorly drained soil profiles.

2.2. Zonal Analysis for Wind Turbine Areas

This section presents the reasoning behind the steps taken in preparing and analyzing the data, as well as the tools used for each phase. Our initial step involved importing each data set into QGIS software tool and reproducing them to ensure uniformity in coordinate systems across all layers. Following this, we created base buffer zones for each wind turbine location. Wind turbines are generally constructed with foundations 15 to 25 meters wide, depending on the structure, which are roughly 4 to 5 times larger than the turbine body. In addition to that, there has been a recent trend toward the expansion of wind turbines, which elevates the probability of damage in the case of a superstructure failure (Halter, 2015). Moreover, when placing a turbine, it is important

to consider soil texture and stress distribution, represented by the pressure bulb phenomenon, and ensure foundation stability (Lavanya, 2020). Moreover, the horizontal area impacted by stress distribution can rise 2 to 2.5 times the foundation size influenced by factors like structure weight, foundation size, and soil type, as stated by wind turbine corporations like CNBM International Wind Power (GEO-SLOPE International Ltd).

During the lifespan of a wind turbine tower, the foundation is exposed to not only the static weight of the tower but also the varying and off-center wind forces. These factors influence the stress distribution beneath the foundation, leading to intricate foundation designs, particularly for taller turbines where the foundation size needs to be larger (Shrestha, 2015). To account for potential uncertainties and variations in soil conditions, a cautious approach was taken. Therefore, we chose a buffer zone with a 100-meter radius to address these factors, ensuring a comprehensive and reliable analysis.

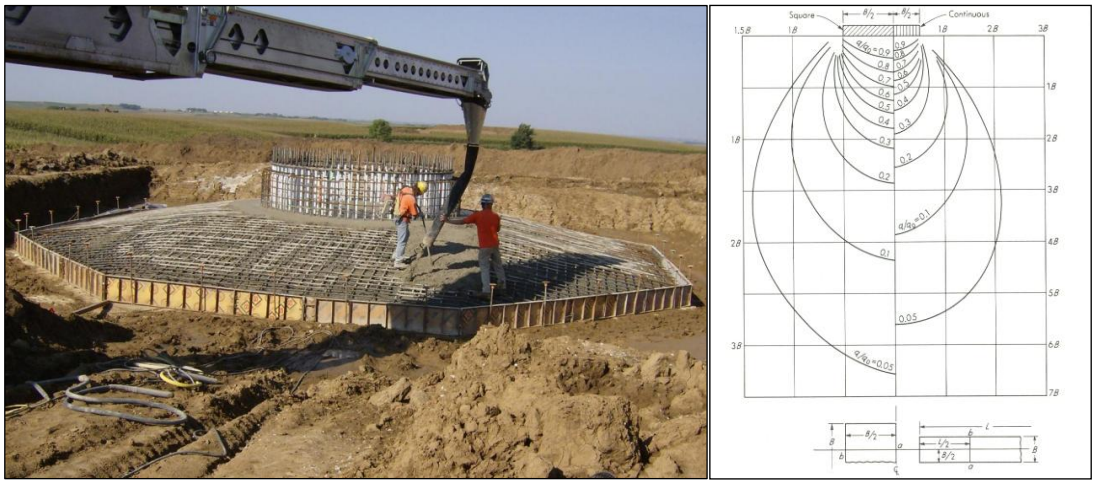

Figure 2. Sample foundation of wind turbine (Ashlock & Schaefer, 2011) and stress distribution isobars of that (GEO-SLOPE International Ltd).

To fully capture the range of elevation changes and flood depths around each wind turbine, we used circular buffer shapes instead of the traditional square or rectangular ones. The circular shape lets us include elevation data from all directions around the wind turbine, which gives us a more complete picture of the terrain. By using circular buffers, we consider the spatial variations in terrain features, ensuring that we consider elevation and flood data from every angle in our analysis.

As illustrated in Figure 3, we expanded the buffer zones for wind turbines at various distances (e.g., 100m, 150m, up to 1,000m) using GIS software. This approach is crucial for thoroughly assessing the vulnerability of wind turbines to flooding. It is also essential that these buffer zones remain accessible during flood events to ensure smooth maintenance and repairs. By concentrating on areas with significant elevation changes, particularly those that shift from flat to sloped terrain, this research tackles the important issue of accessibility during floods. Examining the connection between elevation variance and flood risk provides valuable insights

into how different terrain features impact wind turbine susceptibility. As anticipated, turbines in regions with notable elevation changes encounter greater challenges during floods, due to the higher likelihood of inundation in these areas. Understanding these dynamics is key to developing effective strategies to enhance the resilience of wind energy infrastructure in flood-prone areas.

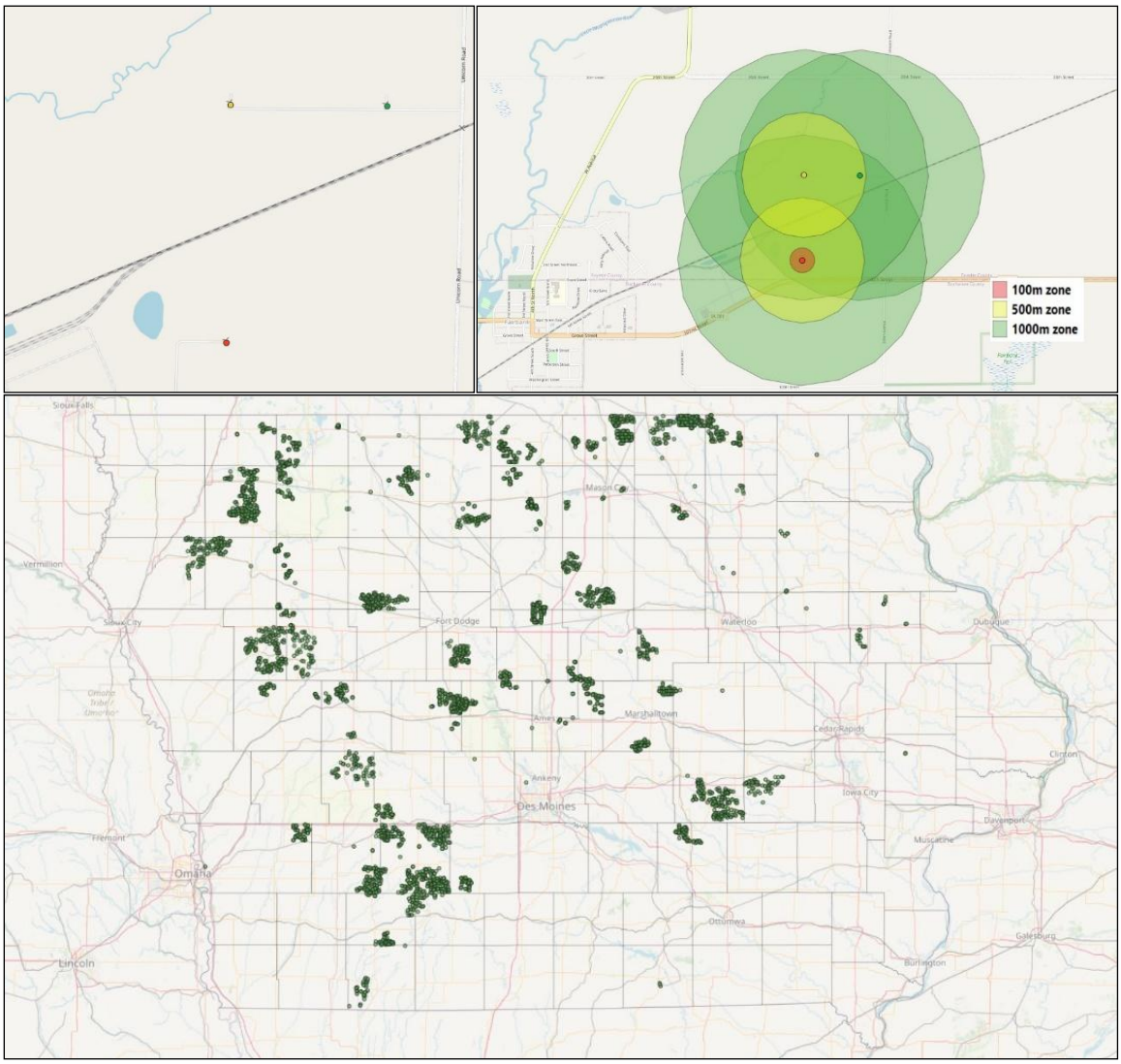

Figure 3. Iowa wind turbine location (upper left), defined sample buffer zones 100, 500, and 1,000m buffer zones (upper right) and distribution of wind turbines in the state with 1,000m buffer zone (lower).

Figure 3 depicts the locations of our wind turbines alongside the expansions of their buffer zones at 100, 500, and 1,000 meters. Additionally, the representation of the 1,000-meter buffer zones serves to underscore the rationale behind these expansions for statewide flood analysis. On the other hand, Figure 4 shows that a small part of the wind turbine buffer zone aggregation and the flood map extension in that area. It can be observed that the flood extents mostly intersect

with the 1,000m buffer zones, as expected, but it also crosses into the 500m and the 100m zones. This highlights the importance of considering all buffer zones in flood risk assessments, as even the smaller zones can be affected, potentially impacting the overall safety and planning for wind turbine sites.

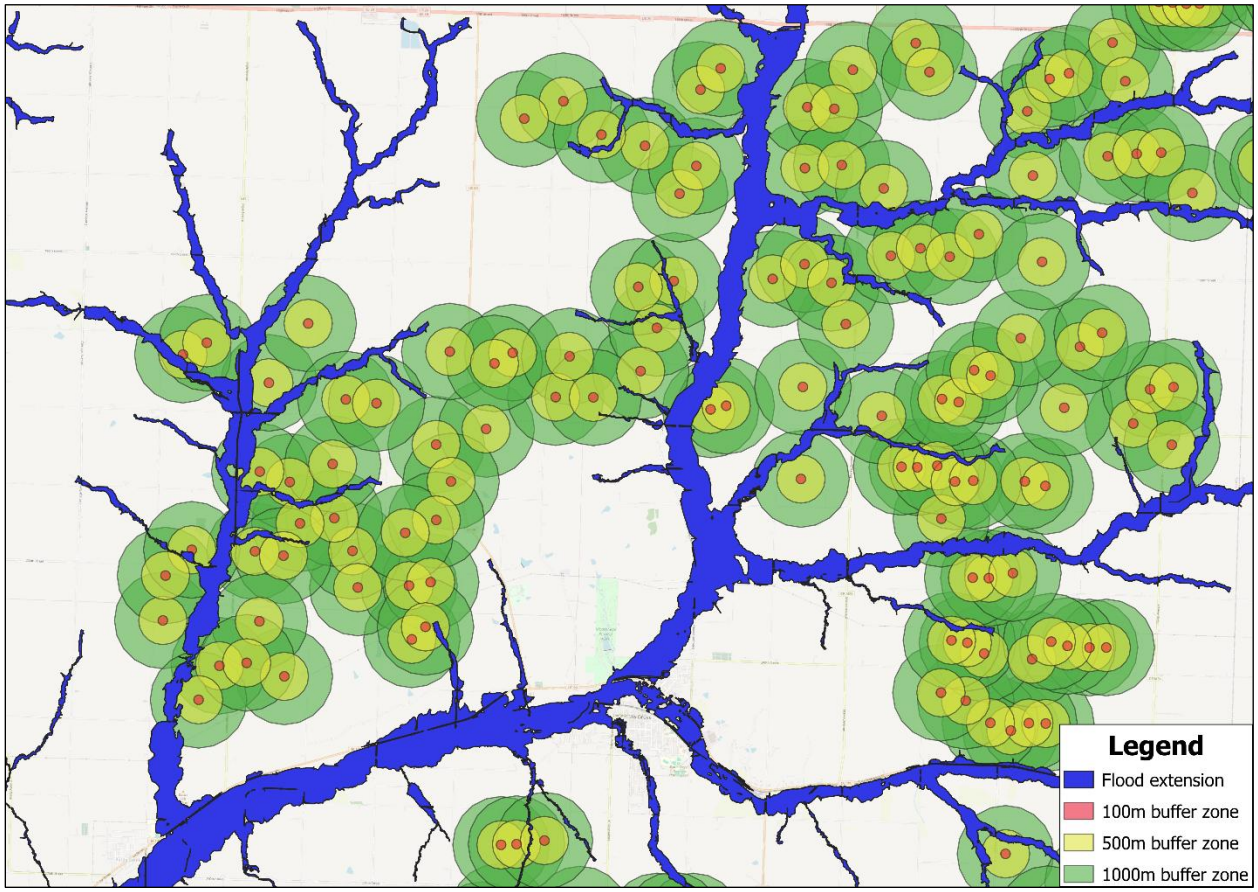

Figure 4. Intersection of 500-year flood extent with various wind turbine buffer zones.

One of the contributing factors to floods and waterlogging is the inadequate infiltration ability and particularly insufficient drainage capacity of surface layers in the landscape (Deasy et al., 2014). In this section, we intersected our turbine locations with the main soil profile raster in Iowa obtained from the Iowa State University database. Subsequently, we extracted the verbal drainage values for each location to examine this critical aspect. The drainage classification, order, and normalized values are detailed in Table 1.

The scoring system reflects this progression, allocating higher scores to soils with superior drainage capacity and lower scores to those with poorer drainage capacity. For instance, excessively drained soils receive higher scores due to their rapid water drainage and minimal water retention capacity, whereas very poorly drained soils, which retain water excessively, are assigned lower scores, often resulting in prolonged waterlogging. This classification system aids

in comprehending the suitability of soil for different purposes, such as agriculture, landscaping, or construction, by evaluating their drainage characteristics (Islam et al., 2024).

Table 1. Drainage capacity classification and drainage score based on capacity order.

Capacity Order	Drainage Capacity Classification	Normalized Drainage Score
1	Excessively drained	1.00
2	Somewhat excessively drained	0.83
3	Well drained	0.67
4	Moderately well-drained	0.50
5	Somewhat poorly drained	0.33
6	Poorly drained	0.17
7	Very poorly drained	0.00

We assign scores to verbal classifications for drainage capacity, ranging from "excessively drained" to "very poorly drained", as can be seen in Table 1, to facilitate correlation calculations with flood vulnerability. While these scores are not formally recognized, they serve as a means of transitioning qualitative data into a quantitative format, aiding in classification and correlation analysis. Detailed explanations of this process are provided within the correlation calculations to ensure understanding.

2.2.1. Zonal Statistics for Wind Turbine Areas

Zonal statistics operate across both raster and vector data, in contrast to numerous geospatial methods that are limited to either raster or vector data exclusively (Haynes et al., 2017). Zonal statistics constitutes the cornerstone of this study, encompassing the computation of summary statistics (e.g., mean, range, variance) for raster data within predefined zones or regions. These zones are typically delineated by vector polygon features, such as administrative boundaries, study areas, or buffer zones surrounding specific features like wind turbines. The primary objective of zonal statistics is to furnish aggregated insights regarding raster datasets within each zone or region of interest. By deriving statistical summaries, zonal statistics empower researchers to analyze spatial patterns, discern trends, and evaluate relationships between raster data and spatial features.

Our study utilizes vector polygon features to define zones or regions of interest, as Figure 5 illustrates. These zones here refer to the circular buffer zones that have been set up around the locations of the wind turbines. The use of circular buffers ensures that we capture the full range of spatial data surrounding each turbine. Once these zones are defined, we extract data from raster datasets such as elevation and flood depth within each zone. We can examine the spatial features of the regions surrounding the turbines thanks to this crucial step.

Once the necessary raster data is extracted, we proceed with calculating key statistical measures like the mean, median, and variance within each buffer zone. These statistics provide

valuable insights into the variability and distribution of the data, allowing us to better understand the terrain and flood risks associated with the wind turbine locations. By analyzing this aggregated data, we can make well-founded conclusions about how spatial factors influence turbine placement and their susceptibility to environmental risks like flooding.

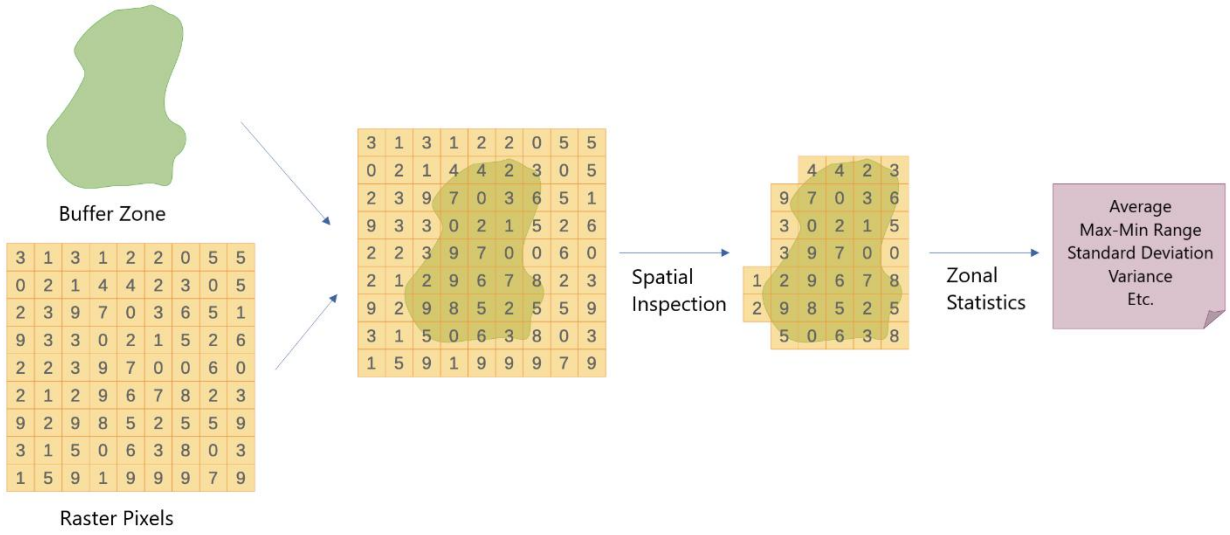

Figure 5. Zonal statistic operation (Saldanha et al., 2024, modified).

In the context of our research, statistical findings are essential for understanding the relationship between elevation variance, flood risk, and wind turbine vulnerability. Here are the statistical findings, their purposes, and the calculations involved:

Mean Elevation: The mean elevation provides an overall measure of the average altitude of the terrain within a given buffer zone around each wind turbine. The mean elevation is calculated by summing up all elevation values within the buffer zone and dividing by the total number of elevation points.

Elevation Range: The elevation range indicates the difference between the highest and lowest elevation points within a buffer zone, providing insight into the topographic relief. The elevation range is calculated by subtracting the lowest elevation value from the highest elevation value within the buffer zone.

Standard Deviation of Elevation: The standard deviation provides a measure of the dispersion of elevation values around the mean. It quantifies how much elevation values deviate from the mean value. As can be seen in Equation 1, the standard deviation of elevation is the square root of the variance:

$$\sigma = \sqrt{\frac{1}{N}\sum_{i=1}^{N}(x_i - \bar{x})^2} \qquad \text{Eq. 1}$$

where x_i is observed value, $\bar{x}$ is mean value and N is number of observations.

Variance of Elevation: The variance of elevation indicates the degree of variability or spread of elevation values within a buffer zone and higher variance suggests greater elevation variation. The variance of elevation is calculated by using Equation 2:

$$Var = \sigma^2 \qquad \text{Eq. 2}$$

To assess flood vulnerability and delineate inundated buffer zones, we utilized the flood depth data for each flood scenario. The analysis was extensive, with 55 raster layers per flood scenario, 6,345 wind turbine locations, and 19 for buffer zone dispersing. we operated zonal statistics tools to extract each location, raster, and zone, maximum flood depth. We employed Python scripts to detect flood-prone areas by retrieving pixels with the maximum depth for an assured method of flood analysis. When multiple flood depth layers permeated into one zone, we used the maximum flood depth value to maintain uniform of flood depth values for the analysis.

We subsequently calculated the statistical parameters, such as the mean elevation, variance, standard deviation, maximum flood depth for flood profiles, and drainage scores for soil profiles. These calculations were done for each location and across expanding buffer zones. This comprehensive approach was essential, as each location exhibited unique characteristics in terms of soil composition, flood risk, and elevation. By aggregating this data, we aimed to develop a broad understanding of the terrain's dynamics, which is critical for informed decision-making.

Following this, we performed a correlation analysis to explore the relationships between elevation variance, flood risk, and wind turbine vulnerability. To aid with data representing the relationship among the variables, we use the Pearson correlation method. This method is suitable for normalized datasets, mostly with no outliers. This indicates a quantitative value and strength for a relationship among variables. The correlation process is demonstrated below in Equation 3, which describes how the Pearson coefficient (r) is calculated:

$$r = \frac{\sum(x_i - \bar{x})(y_i - \bar{y})}{\sqrt{\sum(x_i - \bar{x})^2 \sum(y_i - \bar{y})^2}} \qquad \text{Eq. 3}$$

In this equation, r is the Pearson correlation coefficient, x_i and y_i are individual values for two variables, and $\bar{x}$ and $\bar{y}$ are their respective mean values. The correlation coefficient can range between -1 and 1, with a positive value indicating a direct correlation and a negative value suggesting an inverse relationship. A Pearson correlation coefficient greater than 0.7 is generally considered a strong correlation (Kuckartz et al., 2013).

By using this analysis, we were able to explore how elevation variance, flood risk, and the susceptibility of wind turbines interact. This approach provided clear insights into the dynamics between these variables, offering valuable guidance for future decision-making. Such insights are crucial for creating strategies that will bolster the resilience of wind energy infrastructure in

regions vulnerable to flooding, thereby ensuring that renewable energy remains dependable and effective even when faced with environmental risks.

2.3. Capacity Impact and Future Location Determination

According to the wind turbine dataset, we can determine the wind turbine capacities and potential disruptions during flood scenarios. As previously mentioned, Iowa relies heavily on wind energy (Iowa Environmental Council, 2023), making it crucial to investigate these impacts. The turbine-rated capacity is the output power at the rated wind speed, provided by the manufacturer, ACP, or internet resources, measured in kilowatts (kW).

Out of the 61 wind turbines with no published capacity values, the distribution across different buffer zones is as follows: 5 turbines in the 100m buffer zone, 22 turbines in the 500m buffer zone, and 45 turbines in the 1,000m buffer zone are affected by the 100-year flood scenario. Similarly, 5 turbines in the 100m buffer zone, 23 turbines in the 500m buffer zone, and 48 turbines in the 1,000m buffer zone are affected by the 500-year flood scenario. Despite these limitations with the data, our analysis and the council report show that the impact on total wind production capacity is less than 1%. In the worst-case scenario, where the 1,000m buffer zone is inundated by a 500-year flood, this affects 48 turbines. To ensure consistency, we excluded these turbines from our analysis.

We carried out the location determination of possible wind turbine placement. Our locations should be consistent for flood safety and wind efficiency. First, to get a suitable location, that area should be safe from future flood events for long-lasting feasibility. It is known that these flood periods are based on historic events so due to climate change and global warming, return periods are getting shorter (Mondal & Mujumdar, 2016). That means today’s 500-yr return period may be tomorrow’s 200-yr return period. Thus, it is important to determine this area as flood safe.

Additionally, we have employed 500-year flood selection criteria to identify long-life span locations. To carry on this feature, we extracted the locations that intersected with the 500-year flood scenario extension, and we utilized the remaining -safe- parts. On the other hand, these locations should be efficient for wind speed to provide sufficient power generation capacity. According to the USGS wind turbine database, we have noted that over 82% of wind turbines fall within the 80m to 100m hub height range. To ensure consistency and optimize solutions, we've chosen mean wind profiles at both 80m and 100m levels.

By using the GIS tool, first, we extract the mean wind profile for 80m and 100m and clip it into the Iowa State border. As can be determined from Figure 6, breakpoints of wind profile histograms are 8m/s for 100m height, and 7.5m/s for 80m height. In order to get the proper wind profile, we utilize the places that are exposed to annual mean wind speeds exceeding these breakpoints. Since most of the data in the histograms is concentrated around 7 m/s and 7.5 m/s, selecting a breakpoint slightly above this concentration helps in focusing on the wind speeds that are notably higher than the average. This allows us for a clear distinction between most of the data and the outliers or higher wind speeds.

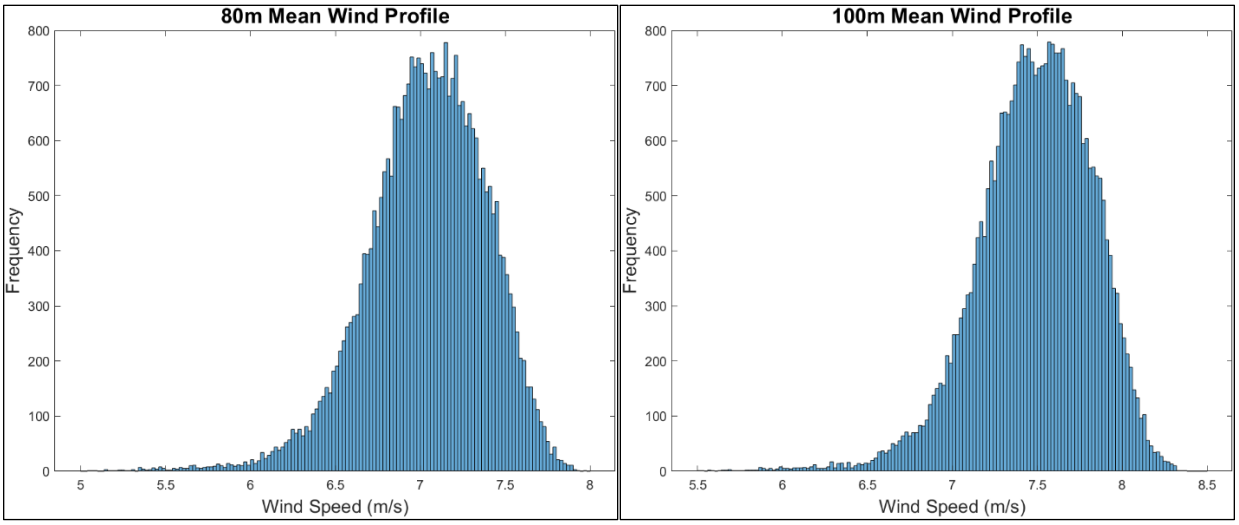

Figure 6. State of Iowa mean wind speed histograms for 80m and 100m height profile.

Lastly, we checked the wind turbine locations to prevent the intersection of these possible locations and existing turbines, we disjointed the existing turbine buffers from our possible location determination analysis. To be on the safe side, we used the 1,000m buffer zone to prevent placement close to the existing wind turbine locations and wind farms because we aimed to determine possible future locations. As a result of this process, we determined 2 sets of possible areas for 2 different wind profile layers (80m and 100m in height), that are suitable for wind turbine placement and safe for flooding, getting proper wind and not occupied by another wind turbine at least 1km from the wind turbine location to closest end of our new proper areas.

3. Results and Discussion

A comprehensive examination of correlation assessments and statistical data reveals important connections between elevation changes, flood risk, wind turbine vulnerability, and drainage capacity in Iowa. This multifaceted study provides a robust foundation for designing mitigation strategies and strengthening wind energy systems against flooding while emphasizing the requirements to consider drainage dynamics in future planning efforts.

3.1. Elevation Analysis for Wind Turbine Areas

Figure 7 shows the average elevation for the different buffer zones, showing critical factors such as mean elevation, range, variance, and standard deviation. This visual representation is a compelling narrative that offers a profound insight into the nuanced tendencies observed within these profiles.

As predicted, the average elevation for buffer zones decreases after the 300-meter expansion. This situation arises from the strategic placement of turbines at higher altitudes, where the surrounding terrain is often excavated for several hundred meters to preserve emergency access to the turbines. As a result, the average elevation ranges between the maximum and minimum points decrease as the buffer zone expansions increase. Since the turbines are positioned at

higher elevations, expanding the buffer zones results in more variation in elevation, which increases the standard deviation, especially noticeable up to the 900-meter expansion. This happens because, although the area covered by the buffer zones grows, the overall range of elevation values stays relatively constant due to the natural limitations of the surrounding terrain.

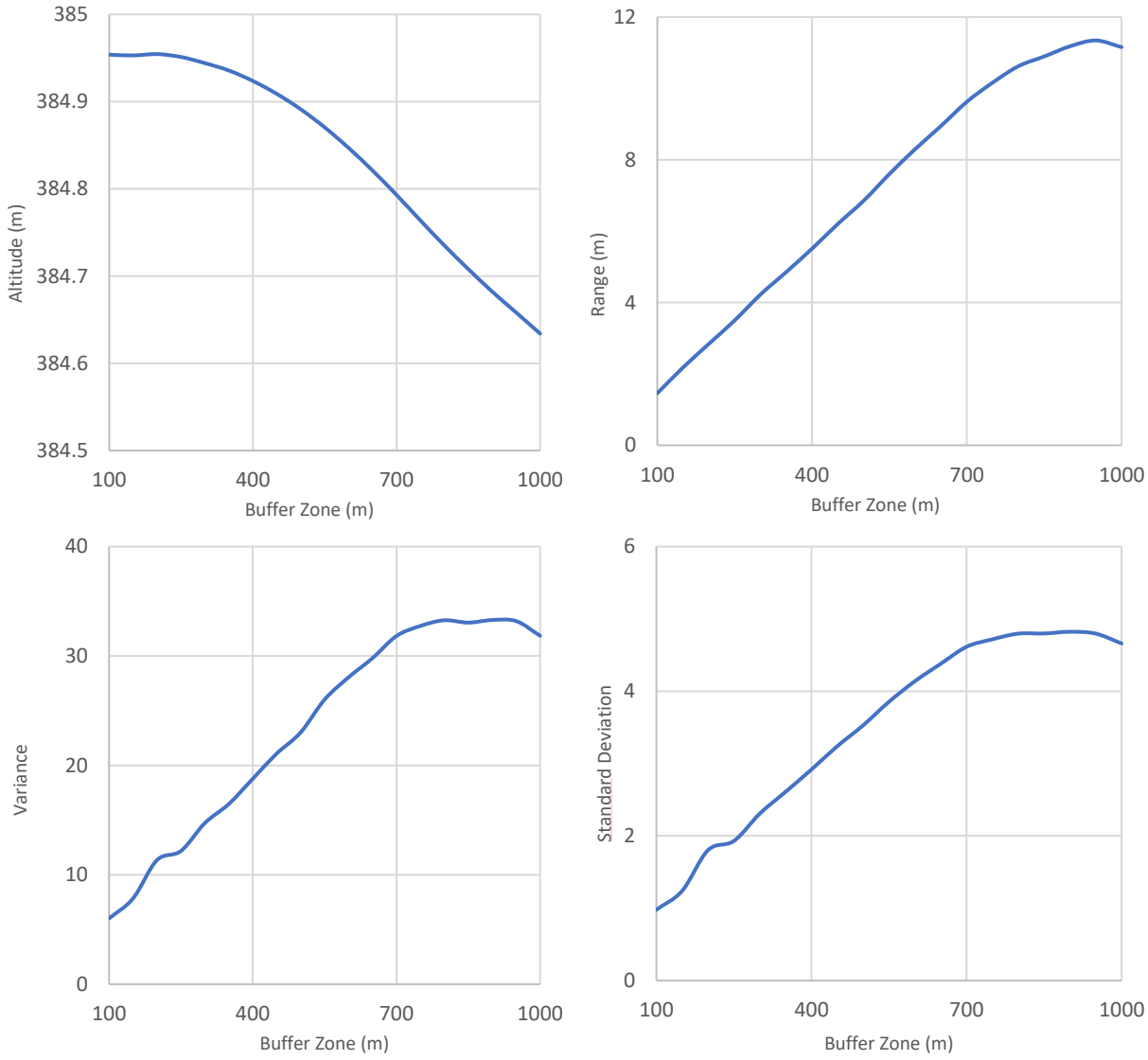

Figure 7. Average Elevation statistics for predefined buffer zones, mean elevation (upper left), elevation range (upper right), elevation variance (lower left), and elevation standard deviation (lower right).

To visually depict the consistency of elevation variation across different buffer zones, we selected the 100, 500, and 1,000m buffer zones statistical values at the same histogram. We utilized MATLAB to create a histogram, and we started at 0.1 variation value instead of 0 to keep the consistency since our raster pixel sizes are 2km x 2km, and when we use 100m radius zone, it is mostly favorable to not intersect the other elevation values, so it became near zero

values. Since we wanted to show the trend, not the exact cumulation, it is more suitable for applying 3 different zones at the same histogram.

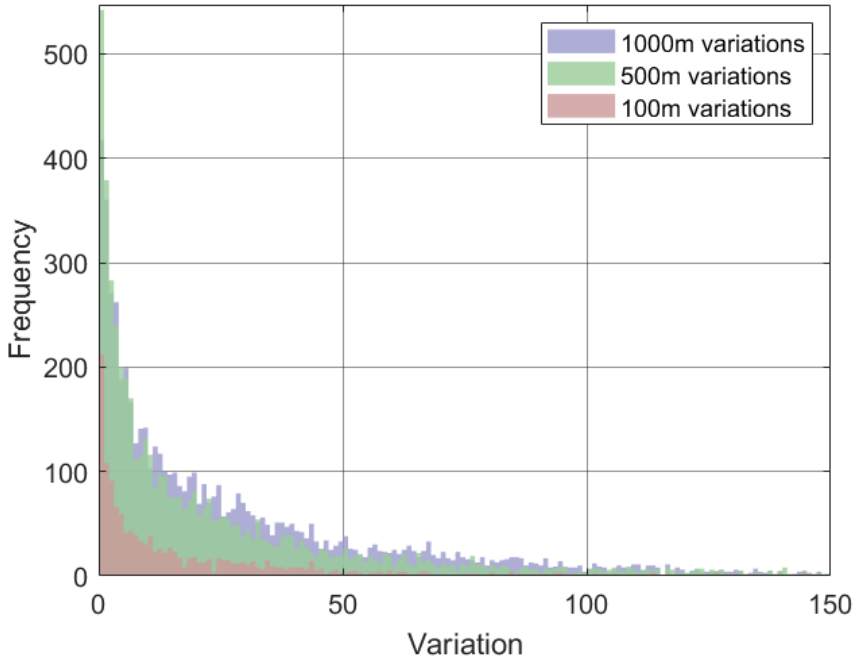

Figure 8. Elevation variation histogram for 1,000m, 500m, and 100m wind turbine buffer zones (0.1-150; 1 interval).

As depicted in Figure 8, wind turbines exhibit a consistent trend of variation increase by expansion across different buffer zones. It is essential to recognize that each location and, consequently, each buffer zone expansion demonstrates unique variations in elevation. While some locations may initially exhibit high variation and subsequently decrease in zonal variations with expanding buffer zones, others may start with low variation (as expected in our study) and then display increased variations. Notably, for our 500m zone variations, although certain values may exceed those of the 1,000m zone varieties, the overall profile of the graphs exhibits remarkable similarity. This consistency underscores the robustness and reliability of the analysis across different buffer zone expansions.

3.2. Flood and Drainage Analysis for Wind Turbine Areas

In our analysis of drainage capacity distribution for the state soil profile, we uncover important insights into how soil permeability and water retention affect flood risk for wind turbine installations in Iowa. By looking at different buffer zones, we focus on key factors like average maximum flood depth, the number of flooded areas, and the average base soil drainage capacity, as shown in Figure 9. This process will assist in understanding the complex relationship between the land's characteristics and the risk of flooding.

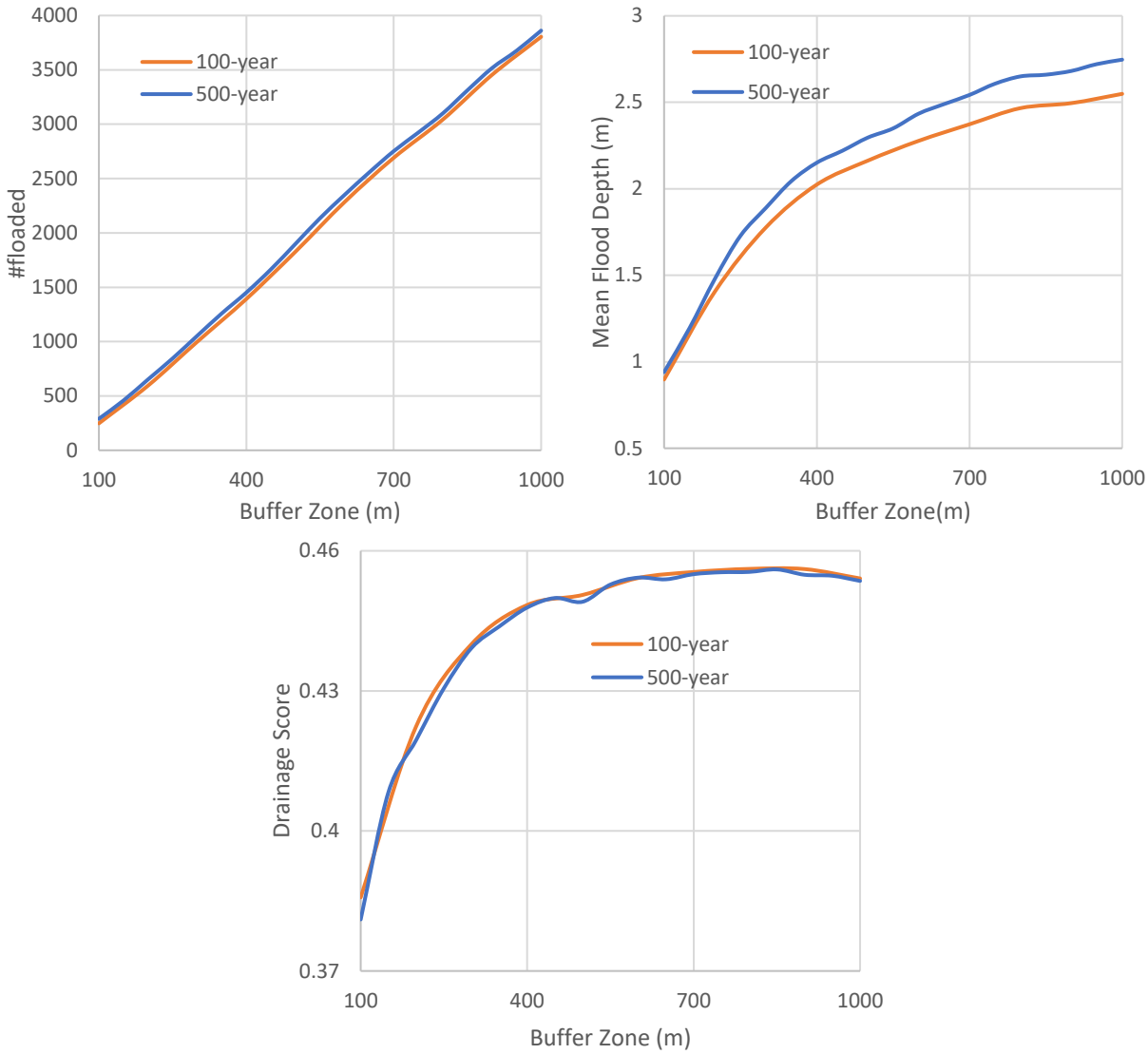

Figure 9. Average maximum flood depth (upper left), number of flooded zones (upper right), and average base soil drainage capacity (lower) for wind turbine buffer zones.

The analysis shows a gradual rise in maximum flood depth as buffer zones extend up to 300 meters, with a curvilinear increase continuing to 1,000 meters. This trend is observed for both 100-year and 500-year flood scenarios, though flood depth and the number of flooded areas is higher for the 500-year scenario across all buffer zones. Similarly, total drainage capacity follows a comparable pattern with buffer zone extension. For both flood scenarios, drainage scores reflect similar trends, though there is a slight decrease in the average drainage score for the 100-year flood scenario beyond the 950-meter buffer zone. This decrease is minor and does not substantially affect the overall analysis, whereas the drainage score remains stable for the 500-year flood zones. Meanwhile, areas with poor drainage were inundated earlier, showing a linear trend in the number of flooded zones. Notably, once the buffer zone expands beyond 850 meters,

more than half of the turbine areas are submerged, emphasizing the urgency for proactive mitigation measures.

3.3. Placement Year Analysis for Wind Turbines

Both the 100-year and 500-year flood scenarios show strong similarities in the distribution of inundation numbers and placement years for wind turbines. The average age of inundated wind turbine areas will be displayed for both scenarios in a single graph in Figure 11. However, the distribution of placement years is nearly identical. So in order to streamline the analysis and avoid redundancy, only the 100-year flood scenario is shown for the distribution of placement years in Figure 10.

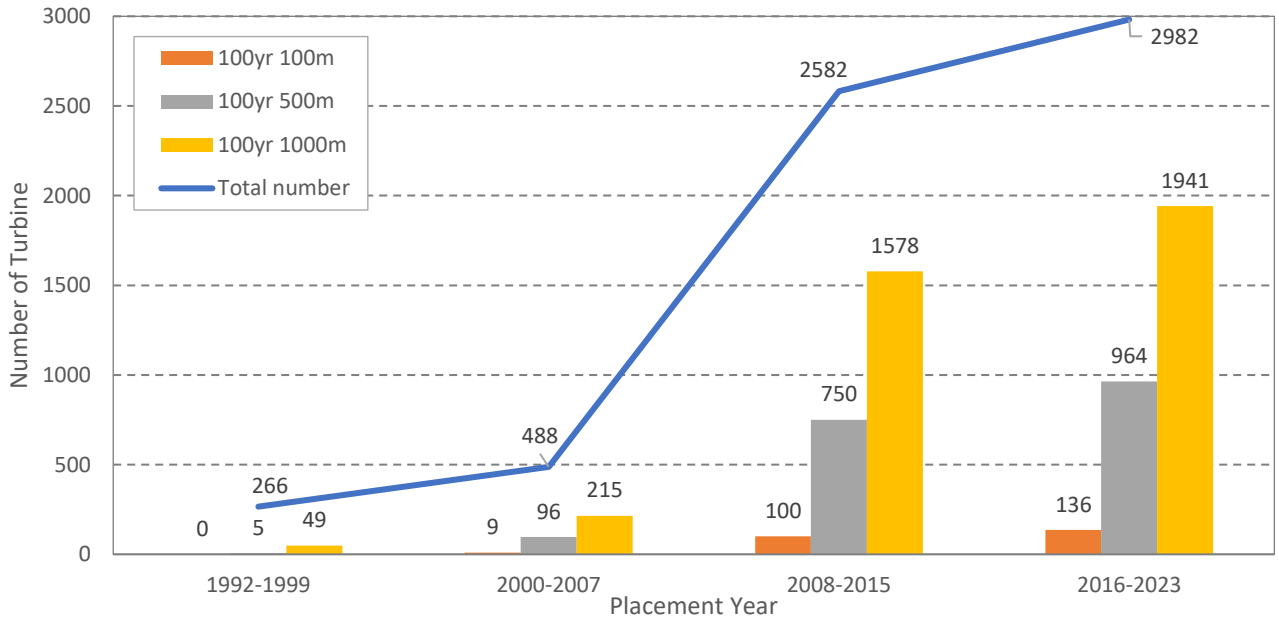

Figure 10. Distribution of placement years for Iowa's wind turbines and their inundation cases under 100-year flood conditions, with 100m, 500m, and 1,000m buffer zone extensions.

As can be seen in Figure 10 and Figure 11, Iowa wind turbines were mostly installed in the last 10 years, and they didn't take the flood vulnerability into account. According to Figure 10, the turbines installed between 2016 and 2023 are particularly at risk, with a notable increase in inundated turbines as buffer zones expand. In addition, Figure 11 indicates that the average age of Iowa wind turbines is 10.68 years, from 100m to 1,000meter extension, both average ages of inundated wind turbines increased from around 8.85 to 9.75 for 100-year and 1,000-year. That means the newer wind turbines are closer to the flood-prone areas than the older ones. Additionally, even at the 1,000m buffer zone, which caused inundation of over 60 percent of the total wind turbines, the average age of inundated turbines is lower than the overall average age so we can indicate again that the newer wind turbines are more likely to be inundated than the old ones.

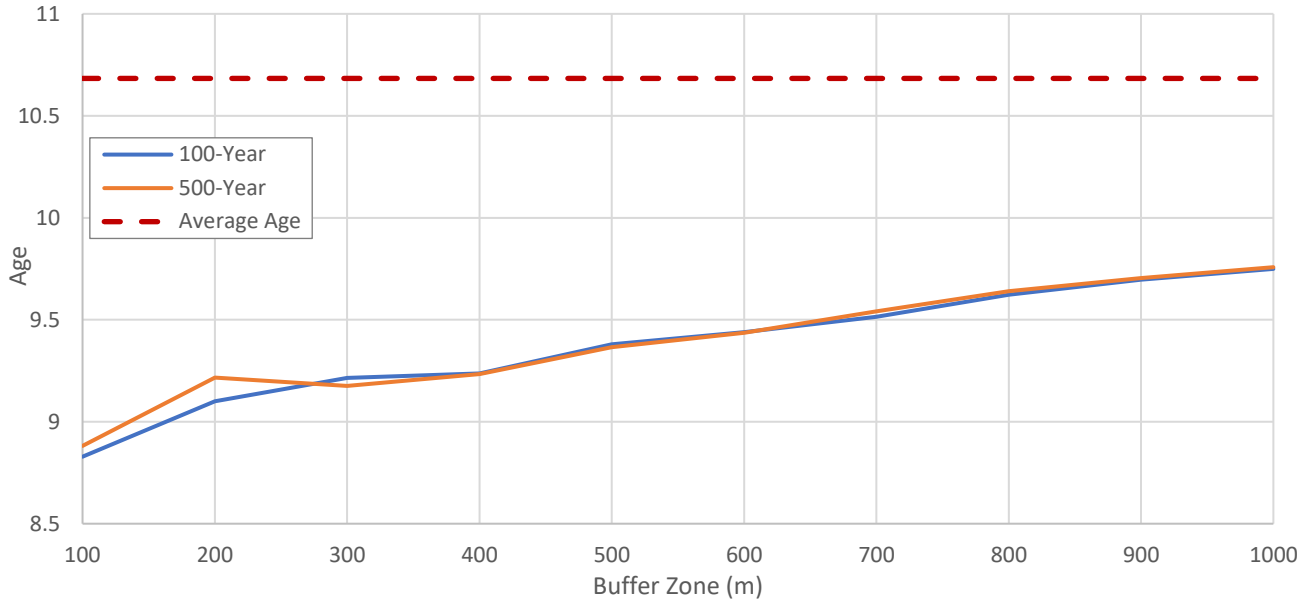

Figure 11. The average age of inundated wind turbine areas for 100-year and 500-year flood scenarios, compared across various buffer zone extensions from the Iowa Wind Turbine Inventory.

3.4. Correlation for Flooding and Terrain Characteristics

In this phase, we investigated the correlations between flood conditions and the related elevation and drainage statistics. Table 2 outlines the complex relationships between flooding and key parameters for wind turbines in Iowa.

Table 2. Pairwise Pearson correlation results for flood vulnerability.

Correlation Pairs	**500-year**	**100-year**
Flood Depth - Elevation Variance	0.966	0.963
Flood Depth – Elevation (σ)	0.974	0.973
Flood Depth - Mean Elevation	-0.816	-0.800
Flood Depth - Drainage	0.950	0.957
Flooded Count - Elevation Variance	0.969	0.962
Flooded Count - Elevation (σ)	0.965	0.959
Flooded Count - Mean Elevation	-0.967	-0.967
Flooded Count - Drainage	0.783	0.778

Evidently, all the correlation values for flooding consistently exceed 0.7 or fall below -0.7, indicating a strong correlation. This finding underscores a notable relationship within the data. Although it is anticipated that larger areas and greater elevation variance would contribute to more flooding, the consistent patterns observed across these variables are particularly significant. The nearly identical profiles enhance the credibility and robustness of our analysis, demonstrating a strong alignment in the results.

3.5. Statewide Inundation Impact Assessment

In Figure 12, we have delineated the inundated areas for the 100m for the 100m, 500m, and 1,000m buffer zones under the 100-year flooding scenario. This visualization assists in illustrating how these zones relate to each other and the extent of flooding. While we analyzed both the 100-year and 500-year scenarios, we decided to visualize only 100-year results since overall distribution remains relatively similar across these flooding scenarios. For instance, in the 100m zone expansion, the difference in inundation between the two flood scenarios is 42 wind turbines, which means a 17% increase. On the other hand, in the 500m zone, the difference is 72 wind turbines, representing a 4% increase, and in the zone of 1,000m, which is our maximum expansion, the difference drops to 52 wind turbines, reflecting only a 1.5% total increase. With over 3,800 wind turbine locations in our case study area, it can be challenging to distinguish the differences due to the accumulation of points.

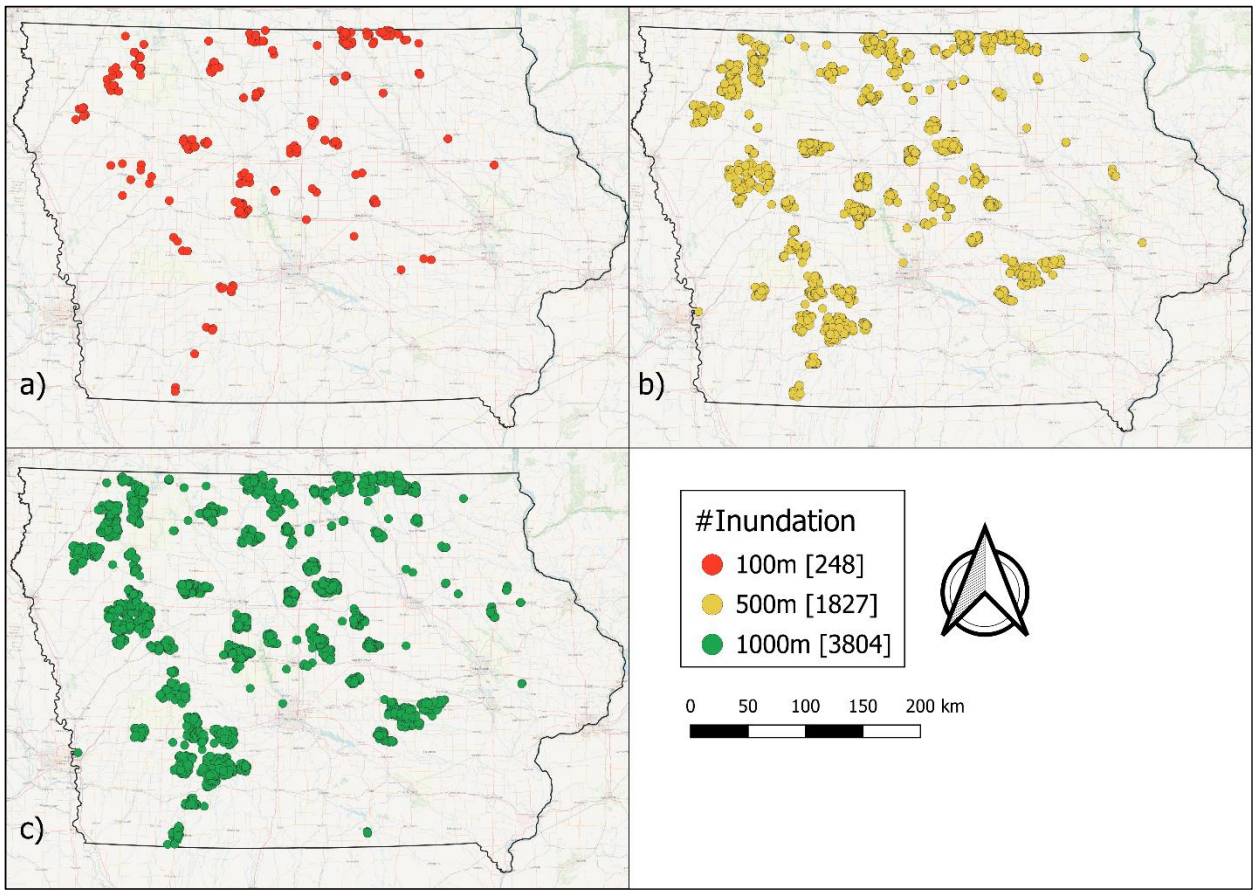

Figure 12. Overall inundated locations for 100m, 500m and 1,000m buffer zone in 100-yr flood scenario of Iowa wind turbines.

As depicted in Figure 12 above, it becomes clear that the northern region of Iowa State is particularly vulnerable to flooding impacts on wind turbines, especially in the smaller buffer zones. When we expand the zone to 500-meter, even higher elevations, especially on the mid-

west side of Iowa, show increased risk due to the significant elevation changes and moderate drainage capacity in the area. In both flood scenarios, about 5 percent of all Iowa wind turbines are affected in the base -100m- buffer zone. This percentage is rising dramatically to 30 percent at the 500-meter extension and a staggering 61 percent with a 1,000-meter extension.

As mentioned earlier, a similar trend appears both in the 100-year and 500-year flood scenarios, highlighting a consistent vulnerability. This pattern underscores a persistent risk, showing that floods are a significant threat to wind turbines in Iowa, regardless of how intense the flooding may be. In the case of capacity disruption, Table 3 illustrates the possible inundation impacts on the energy capacity of Iowa wind turbines. To provide a better understanding of flood impact similarities, 100-year and 500-year data is given for 3 different buffer zone extensions.

Table 3. Possible capacity disruption for 3 different buffer zone extensions (100m, 500m, and 100m) for 2 different flood scenario (100-year, 500-year).

Flood Scenario	**100 Year Flood**			
Zone	**#Inundated**	**%Inundated**	**Capacity Disruption (MW)**	**Capacity Disruption (%)**
100m	248	3.91	536.00	4.20
500m	1827	28.79	3,900.60	30.53
1,000m	3804	59.95	8,004.80	**62.66**
Flood Scenario	**500 Year Flood**			
Zone	**#Inundated**	**%Inundated**	**Capacity Disruption (MW)**	**Capacity Disruption (%)**
100m	290	4.67	626.10	4.90
500m	1899	29.93	4,059.20	31.78
1,000m	3861	60.85	8,118.80	**63.56**

According to the findings provided in Table 3, there is a clear relationship between the capacity disruption scenarios for 100-year and 500-year flood events. The impact of flooding on energy capacity appears to be minor within a 100-meter buffer area, as it only accounts for less than 5% of wind energy capacity in both flood scenarios. However, as the buffer zone size increases, the impact becomes more significant. With a 500-meter buffer area extension, the energy disruption percentage climbs to over 30%, and for a 1,000-meter extension, which is the largest buffer zone we considered, exceeds 60% in both 100-year and 500-year flood scenarios.

Additionally, a consistent pattern emerges across all three sample buffer zone sizes and both flood scenarios. The percentage of capacity disruption is always slightly higher than the percentage of inundated wind turbine zones. This implies that the turbines affected by flooding generally have a higher average energy capacity compared to the turbines that remain unaffected. Although the overall percentage of capacity disrupted is greater than the percentage of inundation, the larger capacities of the inundated turbines amplify the impact. This suggests the necessity of evaluating not just the spatial extent of flooding, but also the potential severity of disruptions in terms of energy capacity.

3.6. Suitable Locations for New Wind Turbine Placement

In this study, we implemented rectangular parcels for evaluating potential wind turbine locations, matching our maximum buffer zone, a 1,000-meter. This dimension was chosen to match the diameter of the largest buffer zone considered, which helps maintain a consistent and systematic analysis approach. Figure 13 presents potential wind turbine sites, focusing on areas with steady wind conditions at altitudes of 80m and 100m. It also excludes regions with existing structures and those at risk of flooding, ensuring that only the most suitable locations are highlighted.

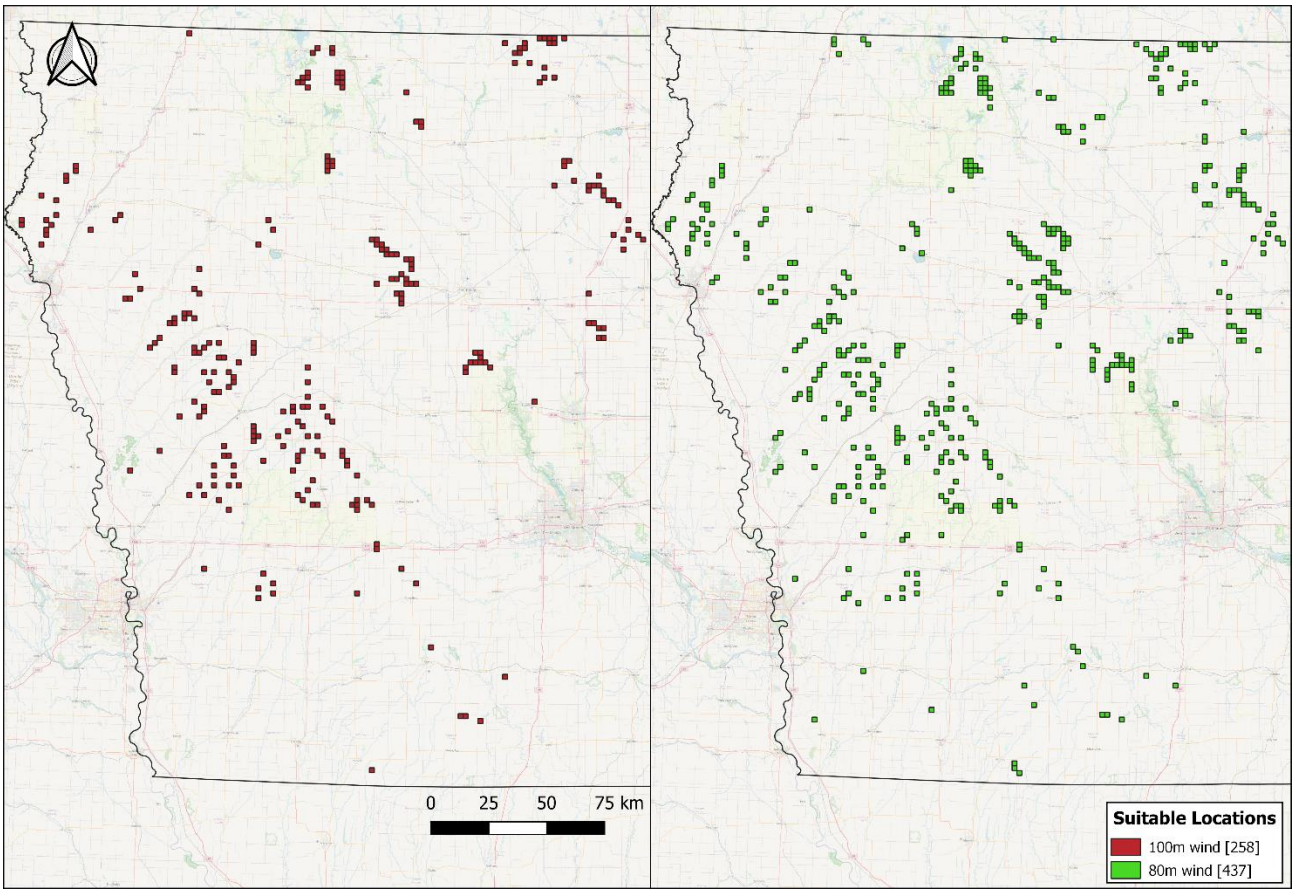

Figure 13. Potential wind turbine locations for steady winds at 100m and 80m altitudes, excluding areas with occupancy and flooding risks.

Despite the west side of Iowa State having a higher density of existing wind turbines, it remains the most suitable area for new installations due to its advantageous elevation, steady wind patterns, and low flood risk. This region is especially effective for wind energy generation because of its stable wind conditions and elevated position. Although there are other potential sites for 80-meter wind turbines, these turbines require lower wind speeds to operate effectively compared to those at 100 meters. Elevating the turbine from 80 meters to 100 meters would increase wind speed by 4.6% and enhance power output by 14% (Lewin, 2010). This indicates that, while placing taller turbines is more complex, it offers substantial advantages in terms of

cost-efficiency and energy production. Our analysis shows that more than 70% of the chosen sites have less elevation variation compared to the average within our 1,000-meter buffer zone. This characteristic further confirms the suitability of these locations for new wind turbine installation, ensuring both stability and efficiency in wind energy production.

4. Conclusion

In summary, this study is very instrumental in offering invaluable insights into how vulnerable wind turbines in Iowa are to flooding, intending to fill the existing gap in knowledge on the resilience of this state's energy infrastructure. Through a careful review of elevation variability, drainage capacity, flood risk, and wind turbine exposure to damage, this work aims to inform the decision-making process that is directed toward resilient improvement in the wind infrastructure of flood-prone areas. Several studies had previously investigated flood risks and wind turbine performances alone in other regions around the world. The scope of this study has thus bridged the gap by jointly considering several environmental parameters to evaluate their combined impacts. By considering at the same time the variance of elevation, flood risk, and vulnerability of wind turbines, we provide a comprehensive approach that depicts complex interrelations between the governing variables.

Through a robust methodology encompassing zonal statistics, correlation analysis, and geospatial mapping, we uncover actionable insights to mitigate the vulnerability of wind turbines to floods in Iowa. Our findings reveal a significant correlation between elevation variance, flood risk, and wind turbine vulnerability, underscoring the need for targeted interventions to bolster resilience. Notably, the visual representations of inundated areas under varying buffer zone expansions highlight the escalating vulnerability of wind turbines to floods as buffer zones extend. From the northern region to the mid-west side of Iowa, the heightened susceptibility of wind turbines underscores the urgency of proactive measures to mitigate flood impact.

Our study on understanding the flood impacts on wind turbine capacity provides insightful information on the relationship between turbine regions and flood risks. As protective buffer zones expand, more turbines are impacted; yet we observed that turbines located in flood-prone regions typically have more energy capacity than the turbines located outside of these zones. Consequently, total energy output can be noticeably reduced even in a rather small area affected by floods. To mitigate this, we applied 500-year flood safety criteria to pinpoint locations for new turbines that are not only resilient to flooding but also positioned to harness efficient wind energy. By incorporating optimal wind speeds at hub heights of 80m and 100m, we identified several promising areas, especially in western Iowa, that meet these conditions without overlapping with existing turbines, ensuring their long-term viability.

In summary, our research contributes scientific understanding while translating findings into actionable strategies to safeguard Iowa's renewable energy infrastructure. By fostering community resilience and promoting sustainability, we support a future where renewable energy remains a cornerstone of Iowa's energy system, resilient against floods and other environmental challenges.

Future research should integrate socioeconomic analyses with environmental assessments to provide a comprehensive view of flood impacts on Iowa's wind energy infrastructure, including factors such as energy capacity and demand. Expanding zonal statistics parameters to incorporate environmental variables like slope, aspect, and land cover types will deepen the understanding of spatial dynamics. Further investigations are needed to analyze turbines that become inaccessible during floods in order to identify vulnerabilities in remote areas. Furthermore, investigating alternative flood scenarios, such as those that occur every 50 years, could provide valuable insights into the resilience of infrastructure and inform adaptive strategies. In addition to conducting detailed performance analyses of turbines at specific sites to optimize placement and guarantee long-term efficiency, future research may also concentrate on the feasibility of installing new turbines by incorporating additional soil and wind turbine inventory data.

5. References

Alabbad, Y., & Demir, I. (2022). Comprehensive flood vulnerability analysis in urban communities: Iowa case study. *International journal of disaster risk reduction*, 74, 102955

Alabbad, Y., Yildirim, E., & Demir, I. (2023). A web-based analytical urban flood damage and loss estimation framework. *Environmental Modelling & Software*, 163, 105670.

Alabbad, Y., Mount, J., Campbell, A. M., & Demir, I. (2024). A web-based decision support framework for optimizing road network accessibility and emergency facility allocation during flooding. *Urban Informatics*, *3*(1), 10.

A.M. Elmoustafa, Neveen Y. Saad, Ehab M. Fattouh, "Defining the degree of flood hazard using a hydrodynamic approach, a case study: Wind turbines field at west of Suez Gulf," Ain Shams Engineering Journal, Volume 11, Issue 3, 2020, Pages 741-749, ISSN 2090-4479, https://doi.org/10.1016/j.asej.2019.12.005.

Borowska-Stefańska, M., Wiśniewski, S., & Andrei, M. T. (2017). Accessibility to places of evacuation for inhabitants of flood-prone areas in Mazovia Province. Geomatics and Environmental Engineering, 11, 31–47.

Cikmaz, B. A., Yildirim, E., & Demir, I. (2023). Flood susceptibility mapping using fuzzy analytical hierarchy process for Cedar Rapids, Iowa. *International journal of river basin management*, 1-13.

Demir, I., Xiang, Z., Demiray, B., & Sit, M. (2022). Waterbench: a large-scale benchmark dataset for data-driven streamflow forecasting. Earth System Science Data Discussions, 2022, 1-19

Draxl, C., B.M. Hodge, A. Clifton, and J. McCaa. 2015. Overview and Meteorological Validation of the Wind Integration National Dataset Toolkit (Technical Report, NREL/TP-5000-61740). Golden, CO: National Renewable Energy Laboratory.

Draxl, C., B.M. Hodge, A. Clifton, and J. McCaa. 2015. "The Wind Integration National Dataset (WIND) Toolkit." Applied Energy 151: 355366.

Duran, E., Alabbad, Y., Mount, J., Yildirim, E., & Demir, I. (2023). Comprehensive Analysis of Riverine Flood Impact on Bridges: Iowa Case Study. *EarthArxiv*, 6434. https://doi.org/10.31223/X5G97H.

GEO-SLOPE International Ltd. (n.d.). Retrieved from http://www.geo-slope.com

Gkritza, K., Smith, D. E., Sperry, R. B., Nlenanya, I., & Jiang, W. (2010). *Iowa's Renewable Energy and Infrastructure Impacts* (No. IHRB Project TR-593). Iowa. Dept. of Transportation.

Grant, C. A., Alabbad, Y., Yildirim, E., & Demir, I. (2024). Comprehensive Assessment of Flood Risk and Vulnerability for Essential Facilities: Iowa Case Study. *Urban Science*, *8*(3), 145.

Grassi, S., Chokani, N., & Abhari, R. S. (2012). Large scale technical and economical assessment of wind energy potential with a GIS tool: Case study Iowa. Energy Policy, 45, 73-85.

Halter, W. R. (2015). Flood Safety on Dikes with Wind Turbines. In *Geotechnical Safety and Risk V* (pp. 516-521). IOS Press.

Haynes, D., Manson, S., & Shook, E. (2017). Terra Populus' architecture for integrated big geospatial services. *Transactions in GIS*, *21*(3), 546-559.

Hoen, B.D., Diffendorfer, J.E., Rand, J.T., Kramer, L.A., Garrity, C.P., and Hunt, H.E., 2018, United States Wind Turbine Database v7.0 (May 10, 2024): U.S. Geological Survey, American Clean Power Association, and Lawrence Berkeley National Laboratory data release, https://doi.org/10.5066/F7TX3DN0.

Hou, G., Xu, K., & Lian, J. (2022). A review on recent risk assessment methodologies of offshore wind turbine foundations. Ocean Engineering, 264, 112469.

Islam, S. S., Yeşilköy, S., Baydaroğlu, Ö., Yıldırım, E., & Demir, I. (2024). State-level multidimensional agricultural drought susceptibility and risk assessment for agriculturally prominent areas. *International Journal of River Basin Management*, 1-18.

Iowa Environmental Council. (2023). Iowa wind energy fact sheet. Retrieved from https://www.iaenvironment.org.

King, J., A. Clifton, and B.M. Hodge. 2014. Validation of Power Output for the WIND Toolkit (Technical Report, NREL/TP-5D00-61714). Golden, CO: National Renewable Energy Laboratory.

Kuckartz, U., Rädiker, S., Ebert, T., Schehl, J., Kuckartz, U., Rädiker, S., ... & Schehl, J. (2013). Korrelation: Zusammenhänge identifizieren. *Statistik: Eine verständliche Einführung*, 207-237.

Lavanya, C., & Kumar, N. D. (2020). Foundation types for land and offshore sustainable wind energy turbine towers. In *E3S Web of Conferences* (Vol. 184, p. 01094). EDP Sciences.

Lebbe, Mohamed Farook Kalendher and Lokuge, Weena and Setunge, Sujeeva, and Zhang, Kevin (2014) Failure mechanisms of bridge infrastructure in an extreme flood event. In: Proceedings of the *1st International Conference on Infrastructure Failures and Consequences*, 16-20 July 2014, Melbourne, pp124-132. ISBN: 978-0-9925570-1-0

Leenaers, H., & Okx, J. P. (1988). "The Use of Digital Elevation Models for Flood Hazard Mapping." Revised 12 December 1988.

Lewin, T. (2010). *An investigation of design alternatives for 328-ft (100-m) tall wind turbine towers* (Master's thesis, Iowa State University). Retrieved from https://doi.org/10.31274/etd-180810-2978

Li, Z., & Demir, I. (2022). A comprehensive web-based system for flood inundation map generation and comparative analysis based on height above nearest drainage. *Science of The Total Environment*, 828, 154420.

Li, Z., Duque, F. Q., Grout, T., Bates, B., & Demir, I. (2023a). Comparative analysis of performance and mechanisms of flood inundation map generation using Height Above Nearest Drainage. *Environmental Modelling & Software*, *159*, 105565.

Li, Z., Xiang, Z., Demiray, B. Z., Sit, M., & Demir, I. (2023b). MA-SARNet: A one-shot nowcasting framework for SAR image prediction with physical driving forces. *ISPRS journal of photogrammetry and remote sensing*, *205*, 176-190.

Lieberman-Cribbin, W., C. Draxl, and A. Clifton. 2014. Guide to Using the WIND Toolkit Validation Code (Technical Report, NREL/TP-5000-62595). Golden, CO: National Renewable Energy Laboratory.

Martinez, A., & Iglesias, G. (2021). Wind resource evolution in Europe under different scenarios of climate change characterised by the novel Shared Socioeconomic Pathways. Energy Conversion and Management, 234, 113961.

McDermott, T. K. (2022). Global exposure to flood risk and poverty. Nature Communications, 13(1), 3529.

Michel, P., Butenweg, C., & Klinkel, S. (2018). Pile-grid foundations of onshore wind turbines considering soil-structure-interaction under seismic loading. *Soil Dynamics and Earthquake Engineering*, *109*, 299-311.

Milligan, M. R., & Factor, T. (2000). Optimizing the geographic distribution of wind plants in Iowa for maximum economic benefit and reliability. Wind Engineering, 24(4), 271-290.

Mondal, A., & Mujumdar, P. P. (2016). Detection of change in flood return levels under global warming. *Journal of Hydrologic Engineering*, *21*(8), 04016021, https://doi.org/10.1061/(ASCE)HE.1943-5584.0001326

Mutel, C. F. (Ed.). (2010). *A Watershed Year: Anatomy of the Iowa Floods of 2008*. University of Iowa Press. https://doi.org/10.2307/j.ctt20mvd5n

Pasqualetti Martin J. (2011). Opposing Wind Energy Landscapes: A Search for Common Cause. Annals of the Association of American Geographers, 101(4), 907–917. https://doi-org.proxy.library.ohio.edu/10.1080/00045608.2011.568879

Peterson, D. A. M., Carter, K. C., Wald, D. M., Gustafson, W., Hartz, S., Donahue, J., Eilers, J. R., Hamilton, A. E., Hutchings, K. S. H., Macchiavelli, F. E., Mehner, A. J., Cajigas, Z. P. P., Pfeiffer, O., & Van Middendorp, A. J. (2019). Carbon or cash: Evaluating the effectiveness of environmental and economic messages on attitudes about wind energy in the United

States. Energy Research & Social Science, 51, 119–128. https://doi-org.proxy.library.ohio.edu/10.1016/ j.erss.2019.01.007

Porté-Agel, F., Bastankhah, M., & Shamsoddin, S. (2020). Wind-turbine and wind-farm flows: a review. Boundary-layer meteorology, 174(1), 1-59.

Rezaei-Shouroki, M. (2017). The location optimization of wind turbine sites with using the MCDM approach: A case study. Energy Equipment and Systems, 5(2), 165-187.

Sadler, J. M., Haselden, N., Mellon, K., Hackel, A., Son, V., Mayfield, J., ... & Goodall, J. L. (2017). Impact of sea-level rise on roadway flooding in the Hampton Roads region, Virginia. Journal of Infrastructure Systems, 23(4), 05017006. https://doi.org/10.1061/(ASCE)IS.1943-555X.0000397

Saldanha, R., Akbarinia, R., Pedroso, M., Ribeiro, V., Cardoso, C., Pena, E. H., ... & Porto, F. (2024). Zonal statistics datasets of climate indicators for Brazilian municipalities. Environmental Data Science, 3, e2.

Sanchez Gomez, M., & Lundquist, J. K. (2020). The effect of wind direction shear on turbine performance in a wind farm in central Iowa. *Wind Energy Science*, *5*(1), 125-139.

Shrestha, Shweta, "DESIGN AND ANALYSIS OF FOUNDATION FOR ONSHORE TALL WIND TURBINES" (2015). *All Theses*. 2291. https://open.clemson.edu/all_theses/2291

Sit, M., Seo, B. C., & Demir, I. (2021). Iowarain: A statewide rain event dataset based on weather radars and quantitative precipitation estimation. *arXiv preprint arXiv:2107.03432*.

Tanir, T., Yildirim, E., Ferreira, C. M., & Demir, I. (2024). Social vulnerability and climate risk assessment for agricultural communities in the United States. Science of The Total Environment, 908, 168346.

USGS. (2010). Floods of May 30 to June 15, 2008, in the Iowa River and Cedar River Basins, Eastern Iowa. Retrieved from https://pubs.usgs.gov/of/2010/ 1190/pdf/of2010-1190.pdf

Yildirim, E., Just, C., & Demir, I. (2022). Flood risk assessment and quantification at the community and property level in the State of Iowa. *International journal of disaster risk reduction*, 77, 103106.

Yildirim, E., Alabbad, Y., & Demir, I. (2023). Non-structural flood mitigation optimization at community scale: Middle Cedar Case Study. *Journal of environmental management*, *346*, 119025.

Zhang, Y., Han, J., Pan, G., Xu, Y., & Wang, F. (2021). A multi-stage predicting methodology based on data decomposition and error correction for ultra-short-term wind energy prediction. Journal of Cleaner Production, 292, 125981.